Printed ISSN 1330–0008
Online ISSN 1333–9125
CD ISSN 1333–8390
CODEN FIZAE4

EXCITON STATE IN A QUANTUM DOT

S. A. SAFWAN, M. H. HEKMAT and N. A. EL-MESHAD

Theoretical Physics Department, National Research Center Cairo, Egypt

Received 21 December 2005; Accepted 21 November 2006
Online 22 May 2007

The exciton binding energies in finite-potential quantum dot discs of GaAs are obtained and the eigenstates and the eigenvalues of the exciton are calculated. We present the exciton binding energy for different values of the disc radius (R) and the disc half-width ($L/2$). The exciton-state stability for large and small sizes of the dot is discussed. We compare our results with the existing theoretical and experimental results. Our results give good estimates for the optimal quantum dot disc geometry, and represent useful data in studies of the optical properties of quantum dots in nano-scale devices.

PACS numbers: 73.61.-r, 85.30.Vw UDC 538.915

Keywords: quantum dot disc, GaAs, finite potential, exciton binding energy, eigenstates, eigenvalues

1. Introduction

The appearance of a peak in the absorption curve of direct-gap materials, such as GaAs, is due to the formation of a complex known as the "exciton". Excitons are elementary excitations in solids and arise due to the Coulomb interaction between electrons and holes. When an excitation energy is transferred to a semiconductor by absorption of a photon, an electron-hole pair is created. At low temperatures, their bound states are formed because the Coulomb interaction between the electron and the hole is prominent. In systems of small dimensions, especially in quantum dots (three-dimensional confinement), the picture is different [1]. Because of nanometer widths and nanometer thickness, and of various shapes, the quantum confinement increases considerably. Whereas the micro-crystallites are approximately spherical, thin discs or cylinders describe better the quantum dots. In quantum dots, the "exciton" (i.e., the confined electron-hole state) remains present even at room temperature in both absorption and emission spectra. Therefore, many devices using exciton transitions have been proposed. These effects are expected to be particularly important when the dimensions of the boxes become comparable to

the excition effective Bohr radius. Although many theoretical studies [10 – 12] have been devoted to the excitonic states in spherical micro-crystals, very few studies consider excitons in cylindrical quantum dots. Up to now, various shapes have been considered, like square flat plates [13 – 14] and cylindrical [15] boxes. In the latter cases, infinite barriers have been used to confine the electron and the hole.

In the present work, we study excitons in quantum discs using a variational approach and the effective-mass approximation with a finite confinement potential. There have been concerns as to whether the effective-mass approximation could still be valid in the quantum dot limit when the size of the exciton could be of the order of the average lattice constant of the bulk semiconductor. Recently, Marin et al. [16] performed variational calculations of the exciton energies for spherical dots of radius in the range of $1.5 - 4$ nm to compare both with experimental and their theoretical data for CdS, CdSe, PbS and CdTe crystallites. They found that the effective-mass approximation is still appropriate for these geometries. Moreover, in the limit of a very small spatial confinement, when the exciton extends substantially into the barrier material, the effective-mass approximation could again be an appropriate approximation with the exciton described by the effective mass of the embedded barrier material (GaAlAs). The paper is organized as follows. In Sec. 2, we present the theoretical model used to describe the exciton in a cylindrical quantum disc. Section 3 presents the results obtained for the exciton binding energy in the quantum dot with a finite barrier, and in Sec. 4 we give the conclusion.

2. Theory

The Hamiltonian [16] of an exciton confined in a QD disc, using the relative coordinates $r = |\bar{r}_{\rm e} - \bar{r}_{\rm h}|$, can be written as

$$\begin{aligned} H &= \frac{-\hbar^2}{2m_{\rm e}^*}\left\{\frac{\partial^2}{\partial r_{\rm e}^2} + \frac{1}{r_{\rm e}}\frac{\partial}{\partial r_{\rm e}} + \frac{r_{\rm e}^2 - r_{\rm h}^2 + r^2}{r_{\rm e} r}\frac{\partial^2}{\partial r_{\rm e}\partial r}\right\} - \frac{\hbar^2}{2m_{\rm h}^*}\left\{\frac{\partial^2}{\partial r_{\rm h}^2} + \frac{1}{r_{\rm h}}\frac{\partial}{\partial r_{\rm h}}\right. \\ &\left. + \frac{r_{\rm h}^2 - r_{\rm e}^2 + r^2}{r_{\rm h} r}\frac{\partial^2}{\partial r_{\rm h}\partial r}\right\} - \frac{\hbar^2}{2\mu}\left\{\frac{\partial^2}{\partial r^2} + \frac{1}{r}\frac{\partial}{\partial r}\right\} - \frac{\hbar^2}{2m_{\rm e}^*}\frac{\partial^2}{\partial z_{\rm e}^2} - \frac{\hbar^2}{2m_{\rm h}^*}\frac{\partial^2}{\partial z_{\rm h}^2} \\ &+ V_{\rm e}(\boldsymbol{r}_{\rm e}, z_{\rm e}) + V_{\rm h}(\boldsymbol{r}_{\rm h}, z_{\rm h}) - \frac{e^2}{\varepsilon\sqrt{r^2 + (z_{\rm e} - z_{\rm h})^2}}\,, \end{aligned} \tag{1}$$

where μ is the reduced exciton mass $\mu = m_{\rm e}^* m_{\rm h}^*/(m_{\rm e}^* + m_{\rm h}^*)$ and ε is the dielectric constant. Assuming a finite potential well, the total confinement potential V for electron or hole is written as

$$V(\boldsymbol{r}_i) = \begin{cases} 0, & r_i < R,\ \ |z_i| < L/2\,, \\ V_0, & \text{otherwise}\,, \end{cases} \tag{2}$$

where i stands for e or h. The full three-dimensional Schrödinger equation for an exciton in a quantum dot is

$$H\Psi(\boldsymbol{r}_{\rm e}, \boldsymbol{r}_{\rm h}, \boldsymbol{r}, z_{\rm e}, z_{\rm h}) = E\Psi(\boldsymbol{r}_{\rm e}, \boldsymbol{r}_{\rm h}, \boldsymbol{r}, z_{\rm e}, z_{\rm h})\,. \tag{3}$$

The Ritz variation principle is used to solve this equation numerically. We are able to determine the ground state by choosing the following trial wave function which takes into account the electron-hole correlation

$$\Psi(\boldsymbol{r}_{\rm e},\boldsymbol{r}_{\rm h},\boldsymbol{r},z_{\rm e},z_{\rm h}) = f(\boldsymbol{r}_{\rm e})f(\boldsymbol{r}_{\rm h})g(z_{\rm e})g(z_{\rm h})\exp\{-\alpha\sqrt{r^2+(z_{\rm e}-z_{\rm h})^2}\}\,. \qquad (4)$$

The variational parameter α is determined by minimizing the value of the exciton energy, and at the corresponding value of α, the exciton energy is

$$E_{\rm ex}(\alpha) = \frac{\langle\Psi|H|\Psi\rangle}{\langle\Psi|\Psi\rangle}\,,$$

where $f(r_i)$ and $g(z_i)$ are the ground wave functions of both the electron and the hole (see our previous paper in Ref. [17]). Thus we have

$$\langle\Psi|H|\Psi\rangle = \int_{-\infty}^{\infty}\int_{-\infty}^{\infty}\int_{0}^{\infty}\int_{0}^{\infty}\int_{0}^{\infty}\Psi^{*}H\Psi\, r_{\rm e}{\rm d}r_{\rm e}\, r_{\rm h}{\rm d}r_{\rm h}\, r{\rm d}r\, {\rm d}z_{\rm e}\, {\rm d}z_{\rm h}. \qquad (5)$$

Substituting the Hamiltonian (1) and the envelope wave function Ψ (4) into the integral (5), and after some tedious algebra, we obtained the following five integrals for the kinetic-energy terms of the Hamiltonian [we used the transformation of variables $(r_{\rm e}, r_{\rm h}, r, z_{\rm e}, z_{\rm h})$ to $(x_{\rm e},\, x_{\rm h},\, x, y_{\rm e},\, y_{\rm h})$]

$$\begin{aligned}
k_1 &= \int_{-\infty}^{\infty}\int_{-\infty}^{\infty}\int_{0}^{\infty}\int_{0}^{\infty}\int_{0}^{\infty}\frac{\hbar^2}{2m_{\rm e}}\frac{1}{R^2}f^2(x_{\rm e})f^2(x_{\rm h})g^2(y_{\rm e})g^2(y_{\rm h})\\
&\quad\times{\rm e}^{-2\alpha\sqrt{R^2x^2+a^2(y_{\rm e}-y_{\rm h})^2}}\left[\left(\frac{f'(x_{\rm e})}{f(x_{\rm e})}\right)^2\right.\\
&\quad\left.+\frac{\alpha R^2(x_{\rm e}^2-x_{\rm h}^2+x^2)}{x_{\rm e}\sqrt{R^2x^2+a^2(y_{\rm e}-y_{\rm h})^2}}\frac{f'(x_{\rm e})}{f(x_{\rm e})}\right]R^8a^2\, x_{\rm e}{\rm d}x_{\rm e}\, x_{\rm h}{\rm d}x_{\rm h}\, x{\rm d}x\, {\rm d}y_{\rm e}\, {\rm d}y_{\rm h},\\
k_2 &= \int_{-\infty}^{\infty}\int_{-\infty}^{\infty}\int_{0}^{\infty}\int_{0}^{\infty}\int_{0}^{\infty}\frac{\hbar^2}{2m_{\rm h}}\frac{1}{R^2}f^2(x_{\rm e})f^2(x_{\rm h})g^2(y_{\rm e})g^2(y_{\rm h})\\
&\quad\times{\rm e}^{-2\alpha\sqrt{R^2x^2+a^2(y_{\rm e}-y_{\rm h})^2}}\left[\left(\frac{f'(x_{\rm h})}{f(x_{\rm h})}\right)^2\right.\\
&\quad\left.+\frac{\alpha R^2(x_{\rm h}^2-x_{\rm e}^2+x^2)}{x_{\rm h}\sqrt{R^2x^2+a^2(y_{\rm e}-y_{\rm h})^2}}\frac{f'(x_{\rm h})}{f(x_{\rm h})}\right]R^8a^2\, x_{\rm e}{\rm d}x_{\rm e}\, x_{\rm h}{\rm d}x_{\rm h}\, x{\rm d}x\, {\rm d}y_{\rm e}\, {\rm d}y_{\rm h},\\
k_3 &= \int_{-\infty}^{\infty}\int_{-\infty}^{\infty}\int_{0}^{\infty}\int_{0}^{\infty}\int_{0}^{\infty}\frac{\hbar^2}{2\mu}\left(\frac{\alpha^2R^2x^2}{R^2x^2+a^2(y_{\rm e}-y_{\rm h})^2}\right)f^2(x_{\rm e})f^2(x_{\rm h})g^2(y_{\rm e})g^2(y_{\rm h})
\end{aligned}$$

$$\times \mathrm{e}^{-2\alpha\sqrt{R^2x^2+a^2(y_\mathrm{e}-y_\mathrm{h})^2}} R^8a^2\, x_\mathrm{e}\mathrm{d}x_\mathrm{e}\, x_\mathrm{h}\mathrm{d}x_\mathrm{h}\, x\mathrm{d}x\, \mathrm{d}y_\mathrm{e}\, \mathrm{d}y_\mathrm{h},$$

$$k_4 = \int_{-\infty}^{\infty}\int_{-\infty}^{\infty}\int_0^{\infty}\int_0^{\infty}\int_0^{\infty} \frac{\hbar^2}{2m_\mathrm{e}}\frac{1}{a^2} f^2(x_\mathrm{e})f^2(x_\mathrm{h})g^2(y_\mathrm{e})g^2(y_\mathrm{h})$$

$$\times \mathrm{e}^{-2\alpha\sqrt{R^2x^2+a^2(y_\mathrm{e}-y_\mathrm{h})^2}} \left[\left(\frac{g'(y_\mathrm{e})}{g(y_\mathrm{e})}\right)^2 - \frac{2\alpha a^2(y_\mathrm{e}-y_\mathrm{h})}{\sqrt{R^2x^2+a^2(y_\mathrm{e}-y_\mathrm{h})^2}}\frac{g'(y_\mathrm{e})}{g(y_\mathrm{e})}\right.$$

$$\left. + \frac{\alpha^2a^4(y_\mathrm{e}-y_\mathrm{h})^2}{R^2x^2+a^2(y_\mathrm{e}-y_\mathrm{h})^2}\right] R^8a^2\, x_\mathrm{e}\mathrm{d}x_\mathrm{e}\, x_\mathrm{h}\mathrm{d}x_\mathrm{h} x\mathrm{d}x\, \mathrm{d}y_\mathrm{e}\, \mathrm{d}y_\mathrm{h},$$

$$k_5 = \int_{-\infty}^{\infty}\int_{-\infty}^{\infty}\int_0^{\infty}\int_0^{\infty}\int_0^{\infty} \frac{\hbar^2}{2m_\mathrm{h}}\frac{1}{a^2} f^2(x_\mathrm{e})f^2(x_\mathrm{h})g^2(y_\mathrm{e})g^2(y_\mathrm{h})$$

$$\times \mathrm{e}^{-2\alpha\sqrt{R^2x^2+a^2(y_\mathrm{e}-y_\mathrm{h})^2}} \left[\left(\frac{g'(y_\mathrm{h})}{g(y_\mathrm{h})}\right)^2 + \frac{2\alpha a^2(y_\mathrm{e}-y_\mathrm{h})}{\sqrt{R^2x^2+a^2(y_\mathrm{e}-y_\mathrm{h})^2}}\frac{g'(y_\mathrm{h})}{g(y_\mathrm{h})}\right.$$

$$\left. + \frac{\alpha^2a^4(y_\mathrm{e}-y_\mathrm{h})^2}{R^2x^2+a^2(y_\mathrm{e}-y_\mathrm{h})^2}\right] R^8a^2\, x_\mathrm{e}\mathrm{d}x_\mathrm{e}\, x_\mathrm{h}\mathrm{d}x_\mathrm{h}\, x\mathrm{d}x\, \mathrm{d}y_\mathrm{e}\, dy_\mathrm{h}.$$

The potential terms take the form

$$p_1 = \int_{-\infty}^{\infty}\int_{-\infty}^{\infty}\int_0^{\infty}\int_0^{\infty}\int_0^{\infty} V_\mathrm{e}(x_\mathrm{e},y_\mathrm{e}) f^2(x_\mathrm{e})f^2(x_\mathrm{h})g^2(y_\mathrm{e})g^2(y_\mathrm{h})$$

$$\times \mathrm{e}^{-2\alpha\sqrt{R^2x^2+a^2(y_\mathrm{e}-y_\mathrm{h})^2}} R^8a^2\, x_\mathrm{e}\mathrm{d}x_\mathrm{e}\, x_\mathrm{h}\mathrm{d}x_\mathrm{h}\, x\mathrm{d}x\, \mathrm{d}y_\mathrm{e}\, dy_\mathrm{h},$$

$$p_2 = \int_{-\infty}^{\infty}\int_{-\infty}^{\infty}\int_0^{\infty}\int_0^{\infty}\int_0^{\infty} V_\mathrm{h}(x_\mathrm{h},y_\mathrm{h}) f^2(x_\mathrm{e})f^2(x_\mathrm{h})g^2(y_\mathrm{e})g^2(y_\mathrm{h})$$

$$\times \mathrm{e}^{-2\alpha\sqrt{R^2x^2+a^2(y_\mathrm{e}-y_\mathrm{h})^2}} R^8a^2\, x_\mathrm{e}\mathrm{d}x_\mathrm{e}\, x_\mathrm{h}\mathrm{d}x_\mathrm{h}\, x\mathrm{d}x\, \mathrm{d}y_\mathrm{e}\, dy_\mathrm{h},$$

$$p_3 = \int_{-\infty}^{\infty}\int_{-\infty}^{\infty}\int_0^{\infty}\int_0^{\infty}\int_0^{\infty} \frac{-e^2}{4\pi\varepsilon\varepsilon_0\sqrt{R^2x^2+a^2(y_\mathrm{e}-y_\mathrm{h})^2}} f^2(x_\mathrm{e})f^2(x_\mathrm{h})g^2(y_\mathrm{e})g^2(y_\mathrm{h})$$

$$\times \mathrm{e}^{-2\alpha\sqrt{R^2x^2+a^2(y_\mathrm{e}-y_\mathrm{h})^2}} R^8a^2\, x_\mathrm{e}\mathrm{d}x_\mathrm{e}\, x_\mathrm{h}\mathrm{d}x_\mathrm{h}\, x\mathrm{d}x\, \mathrm{d}y_\mathrm{e}\, dy_\mathrm{h}.$$

where $a = L/2$, $x_\mathrm{e} = r_\mathrm{e}/R$, $x_\mathrm{h} = r_\mathrm{h}/R$, $x = |x_\mathrm{e} - x_\mathrm{h}|$, $y_\mathrm{e} = 2z/L$ and $y_\mathrm{h} = 2z/L$.

The numerical evaluation of the above integrals gives the expectation value of the Hamiltonian, $\langle H\rangle$, for a certain value of the variation parameter α, from which we obtain $E_\mathrm{b} = E_\mathrm{e} + E_\mathrm{h} - E_\mathrm{ex}$.

3. Results and discussion

For the GaAs material, we used the electron effective mass $m_{\mathrm{e}}^{*} = 0.0667 m_{\mathrm{e}}$, the hole effective mass $m_{\mathrm{h}}^{*} = 0.34 m_{\mathrm{e}}$, the dielectric constant ε equal to 13.18, the band-gap energy $E_{\mathrm{g}} = 1.247\, x_{\mathrm{Al}}$ (x_{Al} is the aluminum concentration) and the ratio between the conduction and the valence band offsets of $65 - 35\%$. The 3D Rydberg energy is equal to $R_y = 0.0044$ eV and the 3D Bohr radius is $a_{\mathrm{B}} = 12.5$ nm.

Figure 1 shows the calculated exciton ground-state binding energy as a function of the radius of the quantum disc for three different values of the half-width $L/2 = 4$, 7 and 10 nm. The calculated values show the presence of the well known peaks of the binding energy curves in nano-structures, which depend strongly on the QD disc radius (R values), but its dependence on the QD disc width is not strong. These results are in a good agreement with the previous data obtained by Le Goff and Stebe [18].

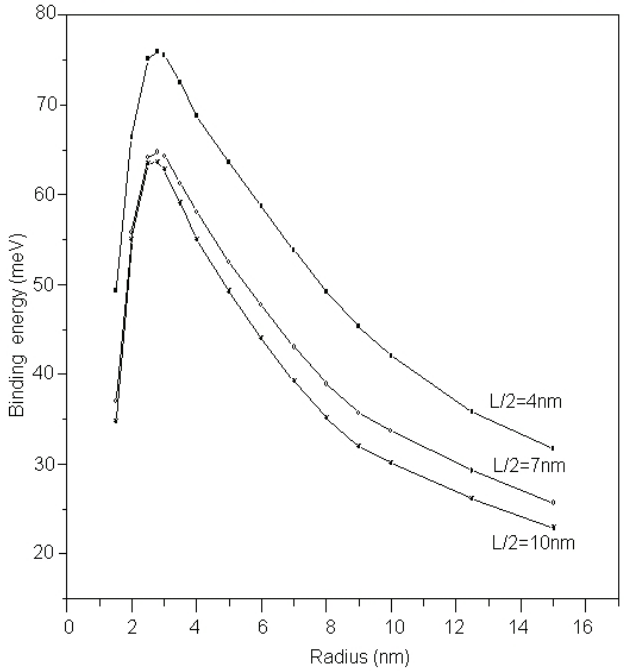

Fig. 1. The binding energy of the exciton as a function of R. The three curves are at different values of QD disc half-width $L/2$ (as indicated). ($x_{\mathrm{Al}} = 0.4$).

Here, we would like to add that the peak positions of the binding energy as a function of $L/2$ occur nearly at the same value of $R = 3$ nm. We notice the sudden decrease of the exciton binding energy when decreasing the value of radius. When R increases from 7 to 10 nm, the binding energy changes almost by 10 meV, and changes by about half of this value if the disc half-width $L/2$ increases from 7 to 10 nm.

Figure 2 displays the variation of the exciton binding energy as a function of R for two different values of Al content ($x_{\mathrm{Al}} = 0.15,\ 0.4$). Here a right shift of the peak position by almost 1 nm, and by 20 meV in the height, is observed when the quantity of Al increases by the factor of about 0.25. The height of the peak is higher due to the increase of the barrier height (larger x) because of the stronger confinement of particles.

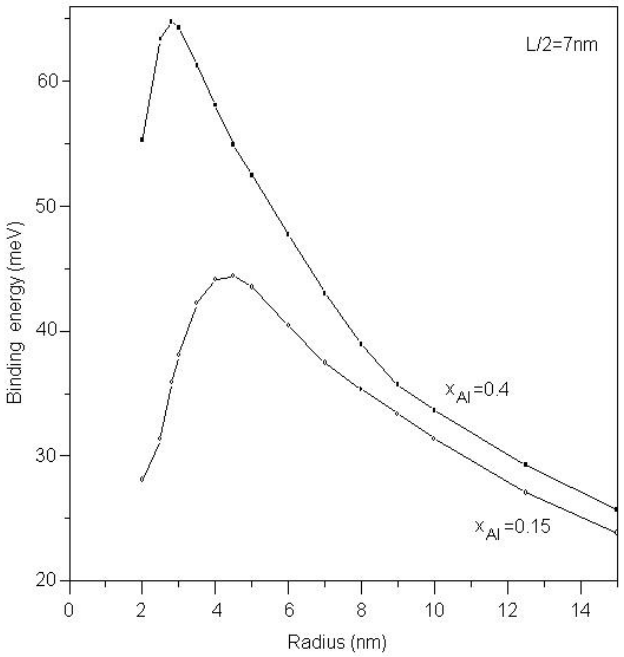

Fig. 2. The variation of the exciton binding energy with R at two different values of Al *concentration, $x_{\mathrm{Al}} = 0.15$ and 0.4.*

The position of the exciton binding energy peaks can be estimated to occur around $L/2 \cong 4$ nm and $R \cong 3$ nm or for diameter $\cong 6$ nm for the quantum dot disc. It has been shown in Ref. [16] that there is a scaling rule for circular and square quantum wires of the form $L/(2R) = 0.9136$, such that a square wire of width L is equivalent to a circular wire of diameter $2R$, if the ratio of 0.9136 is achieved. Using this scaling rule, the critical confinement width for quantum square wire of width $L = 5.4$ nm is equivalent to the present quantum disc with radius $R \cong 3$ nm.

From the behavior of the binding energy positions discussed above, we may conclude that the bulk effect sets in along one spatial axis around $L/2 \cong 4.5$ to 6 nm, fairly independently of the confinement conditions. The present results should be useful for designers of nano-scale devices.

Figure 3 represents the exciton energy E_{ex} as a function of R for $L/2 = 4$, 7 and 10 nm. Again, as we see the exciton energy does not depend strongly on $L/2$, as we mentioned before about the dependence of the binding energy on $L/2$ (Fig. 1).

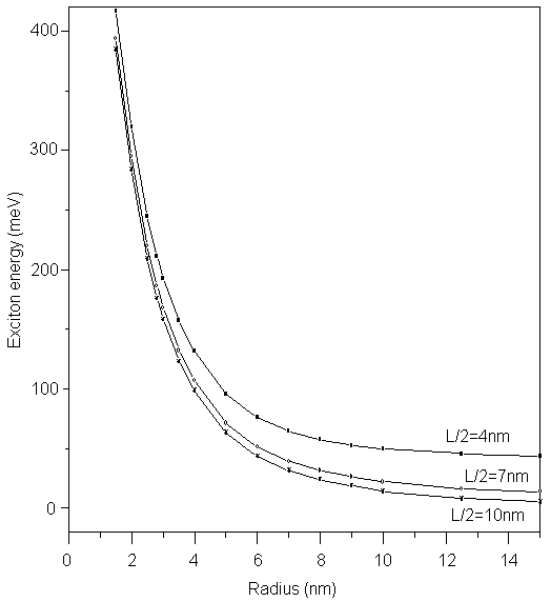

Fig. 3. The exciton energy $E_{\rm ex}$ as s function of R, at the shown values of $L/2$.

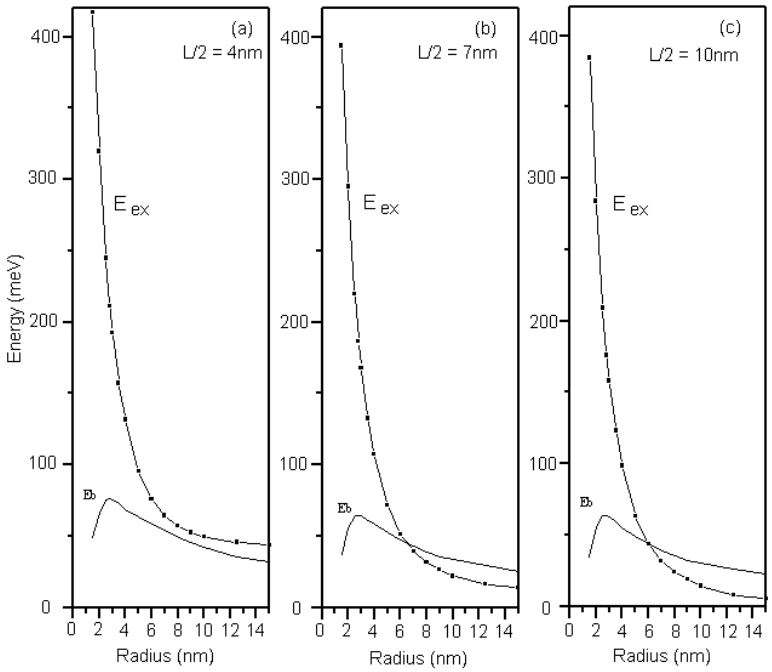

Fig. 4. The exciton energy $E_{\rm ex}$ and the exciton binding energy $E_{\rm b}$ versus the radius R. a) $L/2 = 4$ nm, b) $L/2 = 7$ nm and $L/2 = 10$ nm.

In Fig. 4 we present the exciton binding energy (E_{b}) and the corresponding exciton energy E_{ex} as a function of the disc radius R for three different values of $L/2 = 4$, 7 and 10 nm. In Fig. 4a there is no intersection between the exciton energy and exciton binding energy, $E_{\mathrm{ex}} > E_{\mathrm{b}}$, so a small amount of energy is sufficient to break the combination of the electron-hole pair.

At the intersection points (Figs. 4b and 4c), the binding energy is equal to the expectation value of the Hamiltonian, and is equal to half of the free particle energy ($E_{\mathrm{e}} + E_{\mathrm{h}}$). At energies below the intersection point, where $E_{\mathrm{ex}} > E_{\mathrm{b}}$, the exciton state annihilates faster than above the intersection point where $E_{\mathrm{ex}} < E_{\mathrm{b}}$. The crossover of the binding energy curve with the Hamiltonian curve confirms our above discussion. In order to obtain a large exciton binding energy, we should choose quantum dots with a larger radius (between 3 nm and 10 nm). However, if the radii of quantum dots are beyond the scale of nano-structure, the principle of quantum theory is no longer valid and optical properties of the dots belong to the region of bulk materials.

4. Conclusion

We developed the computer programs to calculate the binding energy of an exciton which is confined in a quantum dot disc of GaAs material. We found that the binding energy depends strongly on the size of the disc. Any change of the Al content of the barrier material affects the exciton confinement in the nano-material. We present theoretical values for several quantum disc dimensions, and we suggest that R should be greater than 3 nm and less than 10 nm. The obtained results are very important in studies of optical properties of the quantum dots and in the nano-scale devices [19,20].

References

[1] L. Esaki, in *Physics and Application of Quantum Wells and Superlattices*, Vol. 170, NATO Advanced Study Institute, series B: Physics, Eds. E. E. Mendez and K. von Klitzing, Plenum Press, New York (1987).

[2] L. Brus, Appl. Phys. A **53** (1996) 465.

[3] L. Brus, IEEE J. Quantum Electron. **22** (1989) 1909.

[4] P. M. Petrof, A. C. Gossard, R. A. Logan and W. Wiegmann, Appl. Phys. Lett. **41** (1982) 635.

[5] O. Brand, L. Tapfer, K. Ploog, R. Bierwolf, M. Hohenstein, F. Phillipp, H. Lage and A. Heberte, Phys. Rev. B **44** (1991) 8043.

[6] T. Tsujikawa, S. Mori, H. Watanabe and M. Yoshita, Physica E **7** (2000) 308.

[7] P. Modak, M. K. Hudait, S. Hardikar and S. B. Krupanidhi, J. Crystal Growth **193** (1998) 501.

[8] K. Kash, A. Scherer, J. M. Worlock, H. G. Craighead and M. C. Tamargo, Appl. Phys. Lett. **49** (1986) 1043.

[9] H. E. G. Arnot, M. Watt, C. M. Sotomayor–Torres, R. Glew, R. Cusco, J. Bates and S. P. Beaumont, Supperlatt. Microstruct. **5** (1989) 459.

[10] C. F. Lo and R. Sollie, Solid State Commun. **79** (1991) 775.

[11] S. I. Pokutnil, Fiz. Tekh. Poluprovodn. **25** (1991) 628 [Sov. Phys. Semicond. **25** (1991) 381].

[12] G. T. Einevoll, Phys. Rev. B **45** (1992) 3410.

[13] G. W. Bryant, Phys. Rev. Lett. **59** (1987) 1140.

[14] G. W. Bryant, Phys. Rev. B **37** (1988) 8763.

[15] Y. Kayanuma, Phys. Rev. B **44** (1991) 13085.

[16] K. S. Tong, F. P. Yuan, X. Xin and H. N. Spector, J. Phys. Cond. Matter **13** (2001) 1485.

[17] M. H. Hekmat, A. Nagwa Elmeshad and S. A. Safwan, Fizika A (Zagreb) **13** (2004) 1.

[18] S. Le Goff and B. Stebe, Phys. Rev. B **47** (1993) 1383.

[19] A. Imamog Lu et al., Phys. Rev. Lett. **83** (1999) 4204.

[20] A. Imamog Lu, Physica E **16** (2003) 47.

EKSITONSKA STANJA U KVANTNOJ TOČKI

Izračunali smo energiju vezanja, svojstvena stanja i svojstvene vrijednosti eksitona u kvantnoj točki s konačnim potencijalom. Opisujemo energiju vezanja eksitona za više vrijednosti polumjera (R) i poluširine ($L/2$) diska. Raspravljamo stabilnost eksitona za male i veće dimenzije diska. Uspoređujemo naše rezultate s poznatim drugim teorijskim i eksperimentalnim rezultatima. Naši rezultati daju dobre ocjene za povoljnu veličinu diska kvantne točke, i predstavljaju korisne podatke za proučavanje optičkih svojstava kvantnih točaka u napravama nano veličine.